AD-A077 911 SCRIPPS INSTITUTION OF OCEANOGRAPHY SAN DIEGO CALIF --ETC F/G 8/10
IS MAGNETIC SECULAR VARIATION RECORDED IN THE OCEAN CRUST: ANAL--ETC(U)
OCT 79 B P LUYENDYK N00014-69-A-0200-6002
UNCLASSIFIED MPL-U-60/79 NL

1 OF 1
AD-
A077911

END
DATE
FILMED
1-80
DDC

LEVEL II (6)

Is Magnetic Secular Variation Recorded in the Ocean Crust: Analysis of Deep Towed Magnetic Anomalies Measured on Cruises Tow Two II and Seven Tow

Bruce P. Luyendyk

Department of Geological Sciences
University of California, Santa Barbara
Santa Barbara, California 93106

Sponsored by the Office of Naval Research Contract N00014-69-A-0200-6002.

SIO REFERENCE 79-20

MPL-U-60/79

1 October 1979

MARINE PHYSICAL LABORATORY

of the Scripps Institution of Oceanography
San Diego, California 92152

SECURITY CLASSIFICATION OF THIS PAGE (When Data Entered)

REPORT DOCUMENTATION PAGE

READ INSTRUCTIONS BEFORE COMPLETING FORM

1. REPORT NUMBER: SIO REFERENCE 79-20	2. GOVT ACCESSION NO.
3. RECIPIENT'S CATALOG NUMBER	
4. TITLE (and Subtitle): 6 IS MAGNETIC SECULAR VARIATION RECORDED IN THE OCEAN CRUST: ANALYSIS OF DEEP TOWED MAGNETIC ANOMALIES MEASURED ON CRUISES TOW ~~TWO~~ II AND SEVEN TOW. Two	5. TYPE OF REPORT & PERIOD COVERED: 9 Summary rept.
	6. PERFORMING ORG. REPORT NUMBER: MPL-U-60/79
7. AUTHOR(s): 10 Bruce P. Luyendyk	8. CONTRACT OR GRANT NUMBER(s): 15 N00014-69-A-0200-6002
9. PERFORMING ORGANIZATION NAME AND ADDRESS: University of California, Santa Barbara, Depart. of Geological Sciences, Santa Barbara, California 93106	10. PROGRAM ELEMENT, PROJECT, TASK AREA & WORK UNIT NUMBERS: 12 28
11. CONTROLLING OFFICE NAME AND ADDRESS: Office of Naval Research, Department of the Navy, 800 N. Quincy, Arlington, Virginia 22217	12. REPORT DATE: 11 1 October 1979
	13. NUMBER OF PAGES: 18 pages
14. MONITORING AGENCY NAME & ADDRESS (if different from Controlling Office): 14 MPL-U-60/79 SIO-REF-79-20	15. SECURITY CLASS. (of this report): UNCLASSIFIED
	15a. DECLASSIFICATION/DOWNGRADING SCHEDULE

16. DISTRIBUTION STATEMENT (of this Report)

Document cleared for public release and sale; its distribution is unlimited.

17. DISTRIBUTION STATEMENT (of the abstract entered in Block 20, if different from Report)

18. SUPPLEMENTARY NOTES

19. KEY WORDS (Continue on reverse side if necessary and identify by block number)

Magnetometer profiles, Gulf of Alaska, statistical and model studies, polarity transitions.

20. ABSTRACT (Continue on reverse side if necessary and identify by block number)

Deeply towed maring magnetometer profiles over anomalies 10 and 9 in the Gulf of Alaska, and number 10 off California, were studied for correlation of short wavelength (short period) features. It is proposed that part of the (dipole) secular variation spectrum is recorded with some fidelity during sea floor spreading. Statistical and model studies suggest that topographic effects are not significant in the data analyzed. Agreement between profiles degenerates at periods shorter than 10^5 years (wavelengths less than 4 km) and coherence tests suggest that a linear system related the earth's field and ocean crust → next page

DD FORM 1 JAN 73 1473 EDITION OF 1 NOV 65 IS OBSOLETE
S/N 0102 LF 014 6601

79 12 11 005

SECURITY CLASSIFICATION OF THIS PAGE (When Data Entered)

217 400

JOB

magnetization only at periods longer than this. One striking observation is that the polarity transitions to anomaly 10 are very shart but the anomaly 9 transition is broad and cannot easily be located in the deep magnetometer profiles.

UNIVERSITY OF CALIFORNIA, SAN DIEGO
MARINE PHYSICAL LABORATORY OF THE
SCRIPPS INSTITUTION OF OCEANOGRAPHY
LA JOLLA, CALIFORNIA 92152

IS MAGNETIC SECULAR VARIATION RECORDED IN THE OCEAN CRUST: ANALYSIS OF DEEP TOWED MAGNETIC ANOMALIES MEASURED ON CRUISES TOW TWO II AND SEVEN TOW

Bruce P. Luyendyk
Department of Geological Sciences
University of California, Santa Barbara
Santa Barbara, California 93106

Sponsored by
Office of Naval Research
N00014-69-A-0200-6002

SIO REFERENCE 79-20

1 October 1979

F. N. SPIESS, DIRECTOR
MARINE PHYSICAL LABORATORY

MPL-U-60/79

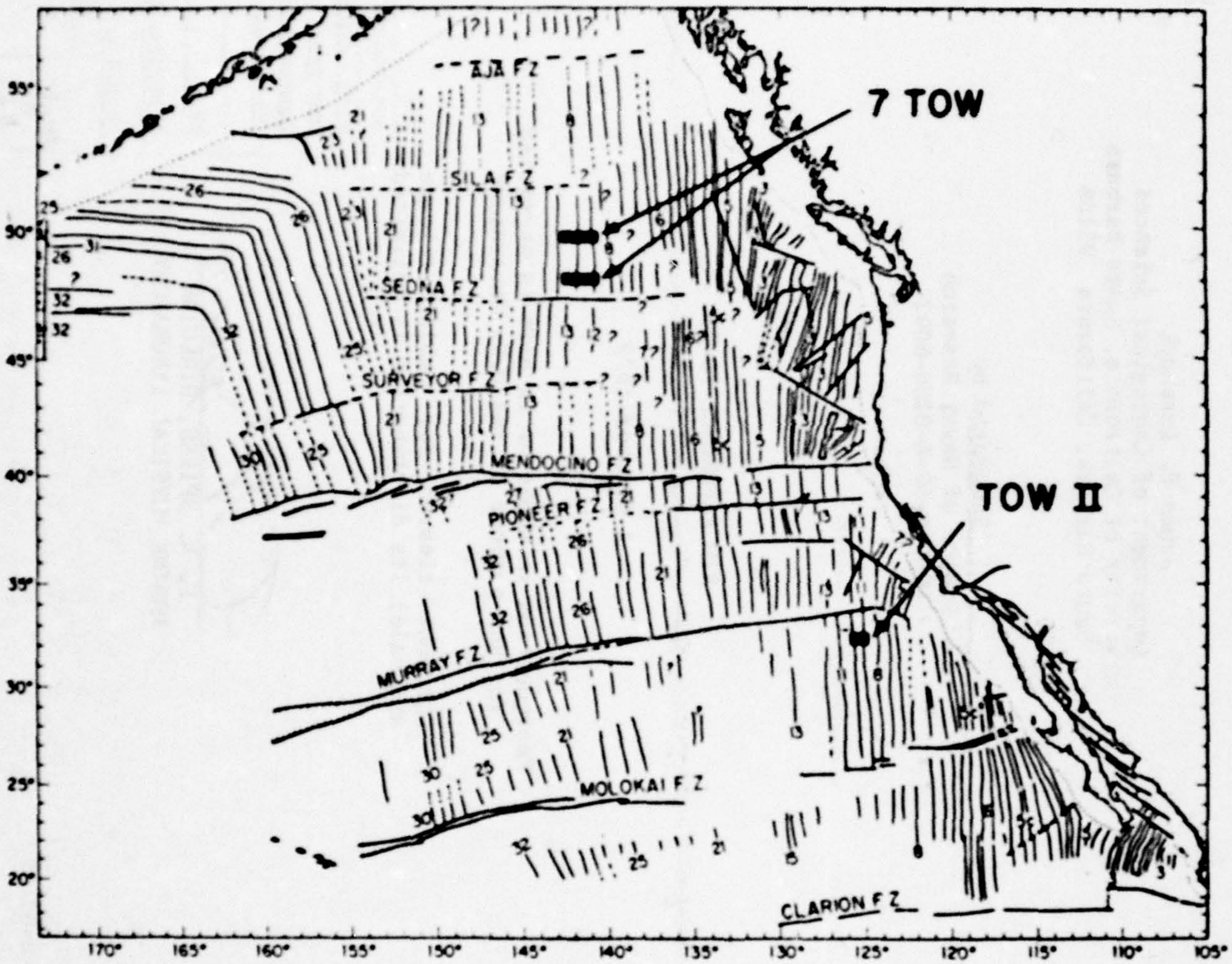

Figure 1. Location of deep magnetometer tows over anomaly 10 and 9 in the northeast Pacific. Base map of numbered anomalies after Menard and Atwater (1968).

IS MAGNETIC SECULAR VARIATION RECORDED IN THE OCEAN CRUST: ANALYSIS OF DEEP TOWED MAGNETIC ANOMALIES MEASURED ON CRUISES TOW TWO II, AND SEVEN TOW

Bruce P. Luyendyk

Department of Geological Sciences
University of California, Santa Barbara
Santa Barbara, California 93106

ABSTRACT

Deeply towed marine magnetometer profiles over anomalies 10 and 9 in the Gulf of Alaska, and number 10 off California, were studied for correlation of short wavelength (short period) features. It is proposed that part of the (dipole) secular variation spectrum is recorded with some fidelity during sea floor spreading. Statistical and model studies suggest that topographic effects are not significant in the data analyzed. Agreement between profiles degenerates at periods shorter than 10^5 years (wavelengths less than 4 km) and coherence tests suggest that a linear system relates the earth's field and ocean crust magnetization only at periods longer than this. One striking observation is that the polarity transitions to anomaly 10 are very sharp but the anomaly 9 transition is broad and cannot easily be located in the deep magnetometer profiles.

PURPOSE

For more than ten years magnetometer profiles have been taken over sea floor spreading magnetic anomalies using the deeply towed instrument package of the Scripps Institution of Oceanography (Spiess and Tyce, 1973). These anomalies have much more spectral energy in shorter wavelengths than equivalent profiles taken on the ocean surface. They have also been shown to be two-dimensional (Luyendyk et al., 1968). These short-wavelength anomalies are due to either, or a combination of, topographic effects (Atwater and Mudie, 1973), field reversals (Luyendyk et al., 1968; Klitgord et al., 1975), petrologic variations (Luyendyk et al., 1968), or secular variation recorded in the crust (Luyendyk, 1969; Larson et al., 1974; Candie and LaBrecque, 1974).

The more controversial interpretation has been that part of the spectrum of the field measured close to the sea floor represents secular variation, most likely of the dipole intensity with a period of about 10^4 to 10^5 years (Larson and Spiess, 1968; Luyendyk, 1969). Secular variation of this type is a global phenomenon like field reversals, whereas non-dipole variation, topographic effects and variation in rock magnetic properties are likely to be local. Therefore, a test of whether dipole secular variation is recorded would be to demonstrate that the same short-wavelength anomalies are seen within the same reversal anomaly from widely separated localities.

Over the years 1967 to 1970 deep magnetometer profiles were collected over magnetic anomaly 10 (about 30 million years old) at two localities in the northeast Pacific (Figure 1). The magnetic profiles obtained showed suggestive short-wavelength correlations.

In this report, statistical and inversion analyses are performed on the data to test the validity and character of these correlations.

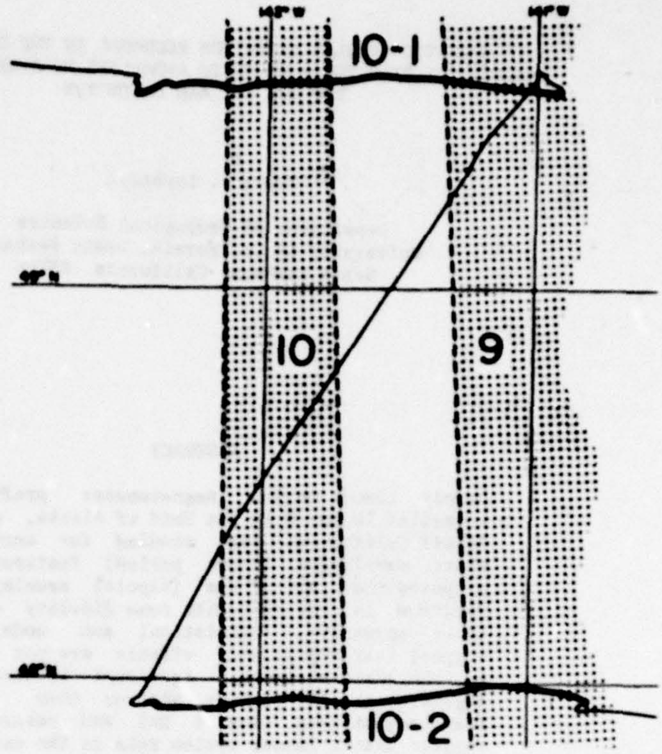

Figure 2. Detail of deep tows over anomaly 10 and 9 in the Gulf of Alaska. Polarity boundaries are picked from surface magnetometer profiles.

FIELD WORK

Deep magnetometer tows over anomaly 10 (Heirtzler et al., 1968) were made off southern California during 1967 on cruise TOW TWO II (T-II2), and in the Gulf of Alaska in 1970 on expedition SEVEN TOW (7 TOW; Spiess et al., 1970; see Figure 1).

On expedition 7 TOW, two long east-west profiles were taken over anomaly 10 and 9. These two profiles are separated by about 165 km in the along strike (north-south) direction. The northerly profile is denoted 10-1 and is 115 km long while the southern one is denoted 10-2 and is 125 km long (Figure 2). Besides the deep magnetometer, a surface magnetometer was towed as well as an airgun. Reflection records are available for half of 10-1 and all of 10-2.

Expedition T-II2 was in an area of abyssal hills off southern California (Luyendyk, 1970). A closely spaced survey was made over the younger positive peak of anomaly 10.

DATA ANALYSES

Gulf of Alaska - 7 TOW

All ship navigation was satellite controlled. The position of the deep magnetometer fish relative to the ship was calculated using program FFIX by knowing the ship position and course, the port-starboard wire angle, and the slant range to the fish and fish depth.

Time series of the total magnetic field, both at surface and at depth, were merged with navigation using program CALCN from Woods Hole Oceanographic Institution, which also removed the IGRF for 1965. The anomaly data are shown in Figures 2 and 3a, b. The magnetometer path was mainly a level flight during both profiles and was an average of 500 meters or more above basement.

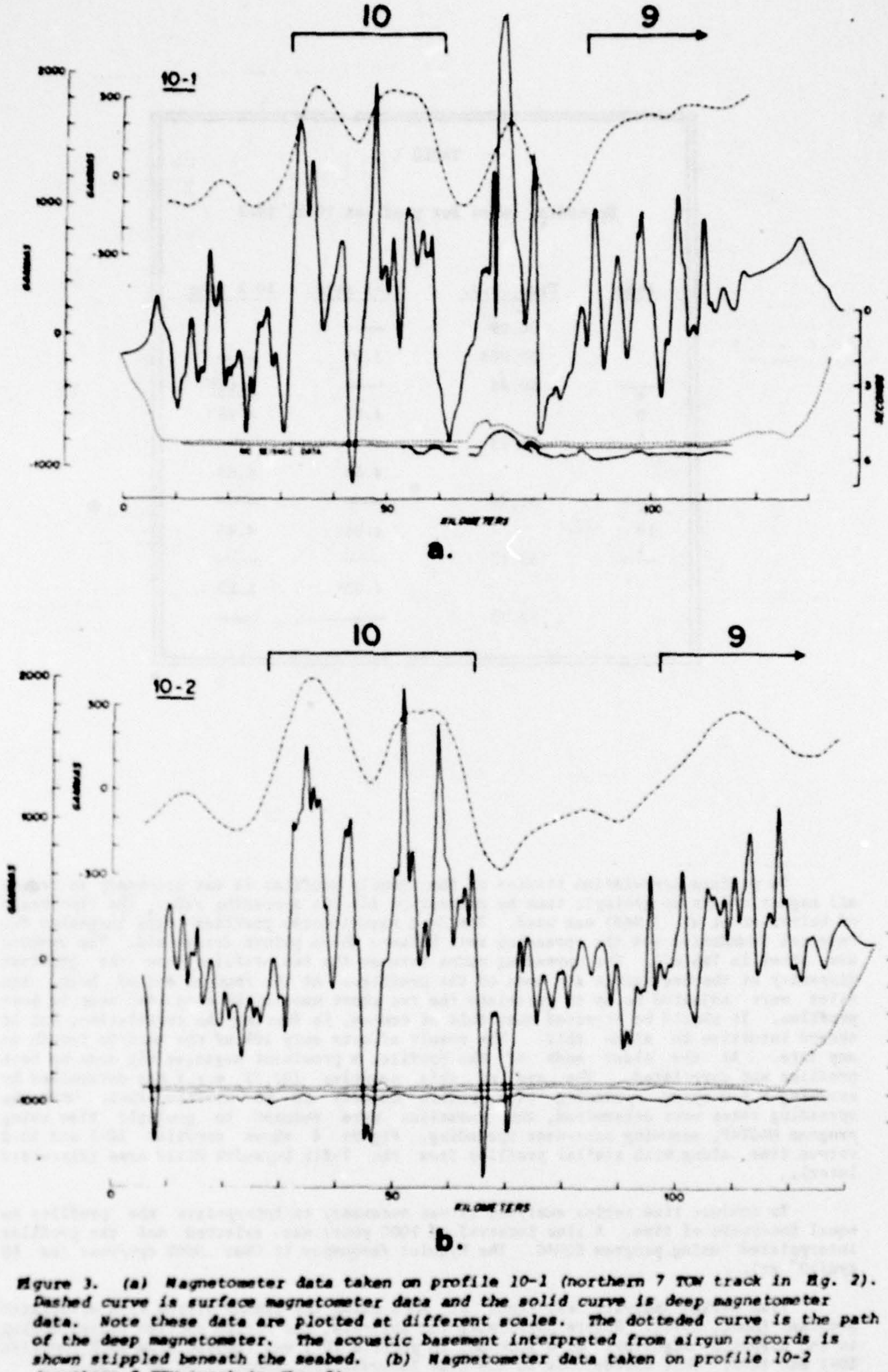

***Figure 3.** (a) Magnetometer data taken on profile 10-1 (northern 7 TOW track in Fig. 2). Dashed curve is surface magnetometer data and the solid curve is deep magnetometer data. Note these data are plotted at different scales. The dotteded curve is the path of the deep magnetometer. The acoustic basement interpreted from airgun records is shown stippled beneath the seabed. (b) Magnetometer data taken on profile 10-2 (southern 7 TOW track in Fig. 2).*

79 12 11 006

TABLE 1

Spreading rates for profiles 10-1, 10-2

Anom	Time, m.y.	10-1 rate	10-2 rate
	30.09		
	30.208	3.9*	
	30.48		6.68*
9		4.63	4.93
	30.93		
		4.68	4.65
	31.50		
10		4.04	4.90
	32.17		
		4.00*	4.53
	32.73		

To perform correlation studies of the anomaly profiles it was necessary to reduce all magnetic data to geologic time by correction for the spreading rate. The time scale of Heirtzler et al. (1968) was used. The deep magnetometer profiles were inspected for reversal boundaries and the spreading rate between these points determined. The results are shown in Table 1. The spreading rates between the two profiles show the greatest disparity at the beginnings and ends of the profiles. At the younger end of both, the rates were adjusted so as to correlate the two short wavelength anomalies seen in both profiles. It should be stressed that this of course, is forcing the correlation, but it seemed intuitive to allow this. The result affects only 10% of the profile length at any rate. At the older ends of the profiles a prominent negative dip seen on both profiles was correlated. The age of this negative (32.73 m.y.) was determined by assuming a 4.0 cy/yr spreading rate before anomaly 10 in profile 10-1. Once the spreading rates were determined, the anomalies were reduced to geologic time using program MAGTRP, assuming east-west spreading. Figure 4 shows profiles 10-1 and 10-2 versus time, along with similar profiles from the T-112 Luyendyk Hills area (discussed later).

To conduct time series analyses it was necessary to interpolate the profiles to equal intervals of time. A time interval of 1000 years was selected and the profiles interpolated using program EQMAG. The Nyquist frequency is thus .0005 cyc/year (or 50 cyc/10^5 yr).

Time series analysis was done at WHOI using the TIMSAN system with associated programs (Hunt, 1977). Before performing the analysis, the record section corresponding to the magnetic signature of a seamount in profile 10-1 was removed from both profiles 10-1 and 10-2. This corresponds to the time interval from about 31.05 to 31.35 m.y.

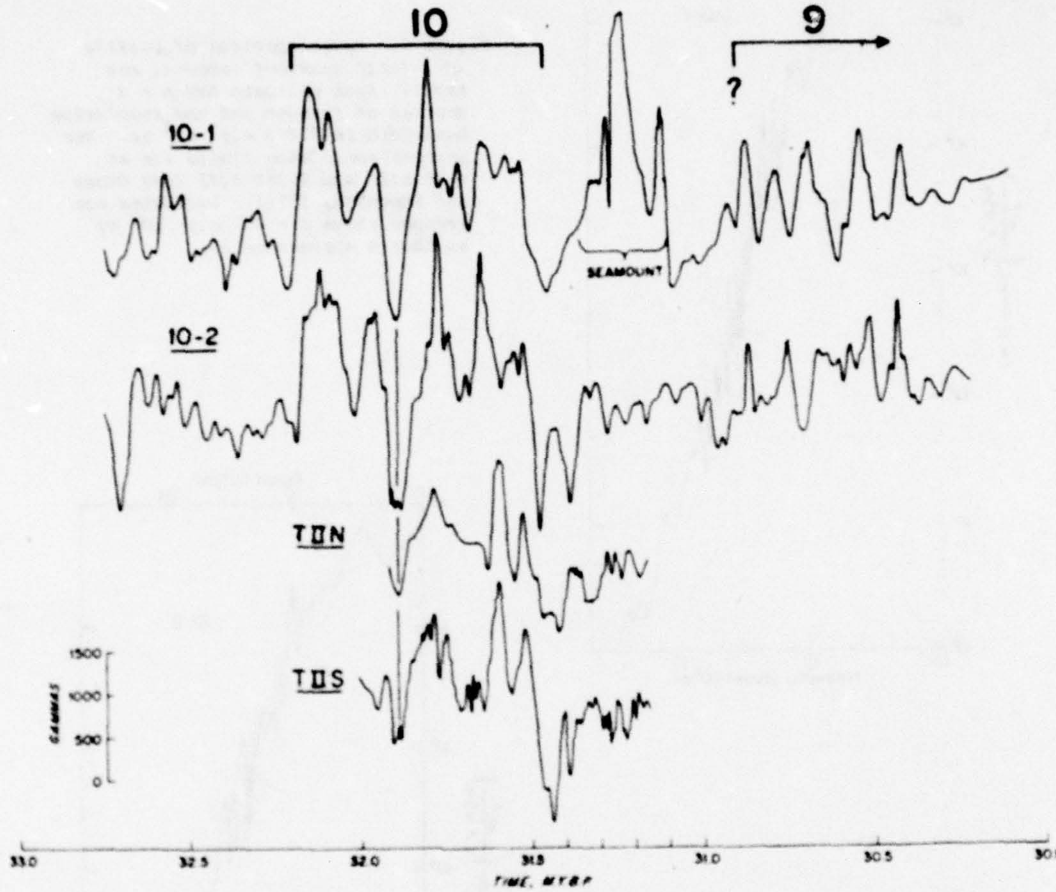

Figure 4. Deep magnetometer profiles taken over anomalies 10 and 9 in the Gulf of Alaska (10-1, 10-2) and off southern California (T-IIN, T-IIS), corrected to geologic time by allowance for spreading rate (Tables 1 and 2. Locations are shown in Figure 1.

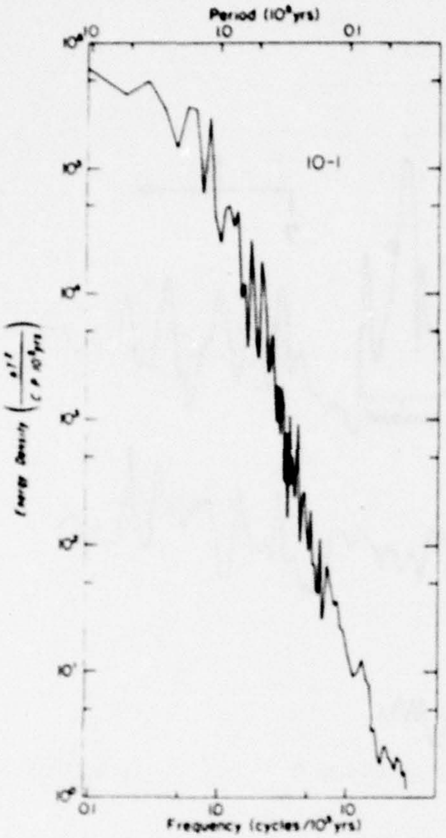

Figure 5. Power spectrum of profile 10-1 (with seamount removed; see text). Each estimate has $n = 4$ degrees of freedom and the resolution bandwidth is 0.093 c.p. 10^5 yr. The percent confidence limits are at 0.26 $S(f)$ and 0.360 $S(f)$ (see Otnes and Enochson, 1978). Estimates are grouped above $f = 3.7$ c.p. 10^5 yr so that n approaches 20.

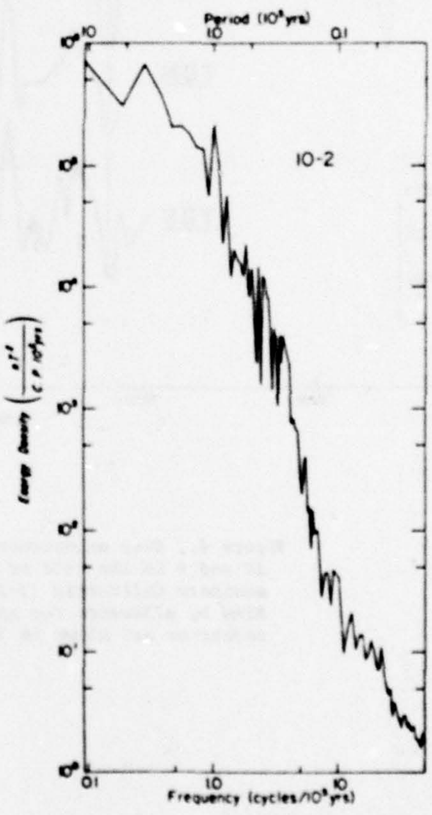

Figure 6. Power spectrum of profile 10-2 (with equivalent time for seamount in 10-1 removed). Same degrees of freedom and confidence limits as Figure 5.

The first analysis step was calculation of power spectra to identify prominent harmonics and to establish background noise levels. Power spectra of both profiles 10-1 and 10-2 (Figures 5 and 6) show most energy concentrated in periods longer than 10^5 years (ca. 4 km) with a sharp decrease at higher frequencies. A noise level is not apparent at higher frequencies. Very possibly there is a peak at 0.5×10^6 years related to the 0.5 m.y. length of anomaly 10.

A power spectrum in wavenumber space was calculated for the anomaly amplitude versus distance in profile 10-2 (Figure 7; calculated within the inversion process described below). A peak centered at 20.5 km is due to the reversals within anomaly 10; peaks at 5.12 and 7.32 km are associated with the short wavelength anomalies superimposed upon the reversal pattern (see Figure 3b).

A visual comparison of the anomaly profiles in Figure 4 suggests several correlations. The low at 31.9 m.y. and peaks at 31.5, 31.6, 31.8, 32.0, and 32.1 m.y. within anomaly 10 are particularly apparent. However, the eye is signficantly influenced by the "square-wave" appearance of anomaly 10. For this reason the time series were band-pass filtered to remove the square-wave due to the reversal boundaries. The filters used were the second degree recursive filters P_3 described by McCullogh (1968) and Stallings (1966). The band-pass transfer function is shown in Figure 8. Random noise was also band-passed through this transfer function to test for ringing

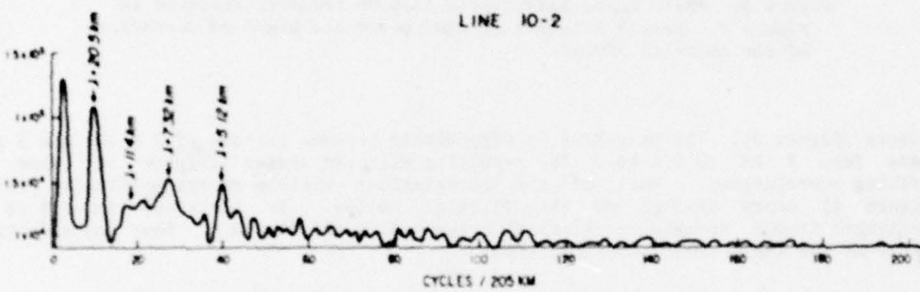

Figure 7. Unsmoothed power spectra of profile 10-2 in spatial dimensions (kms). Confidence limits (95 percent) are at 39.5 S(f) and 0.271 S(f).

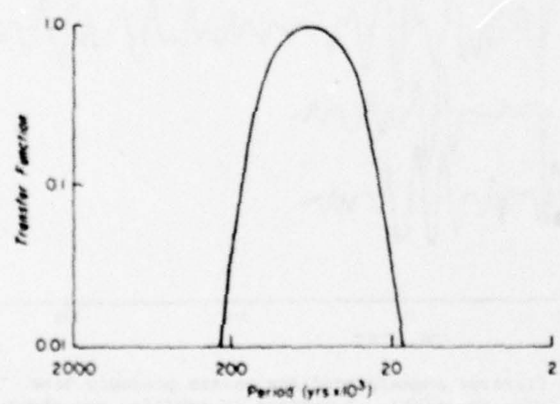

Figure 8. Transfer function for band pass filter used on the deep magnetometer time series; after McCullough (1968).

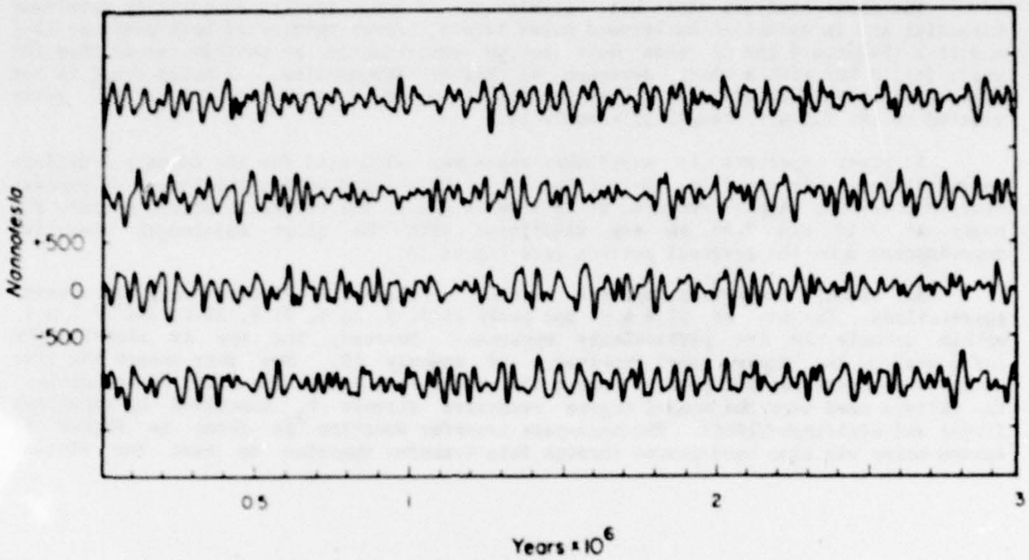

Figure 9. White noise band-passed through transfer function in Figure 8. Sample interval is 1000 years and standard deviation of the noise is 500 nT.

effects (Figure 9). The pass-band is effectively between periods of 2×10^5 and 2×10^4 years (ca. 8 km to 0.8 km). The resulting filtered series (Figure 10) show some striking correlations. Most of the correlations visible on the unfiltered profiles (Figure 4) carry through on the filtered series. In addition, removal of long wavelength trends reveals correlations between 30.5 and 31.0 m.y. Some end effects are likely as the input series were not tapered.

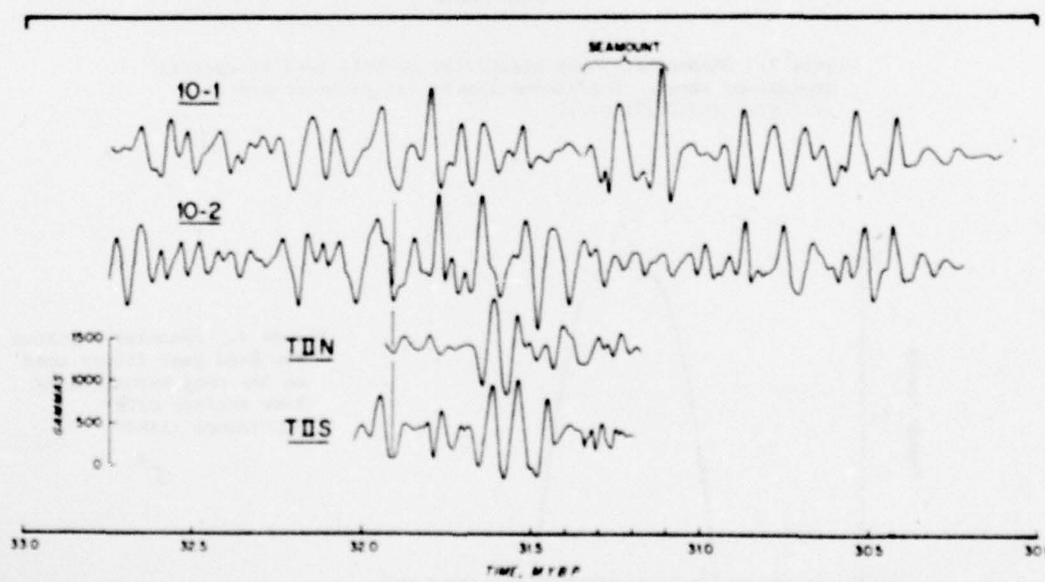

Figure 10. Band-pass filtered anomaly profiles versus geologic time (see Fig. 8 for transfer function). Locations of profiles are shown in Figure 1.

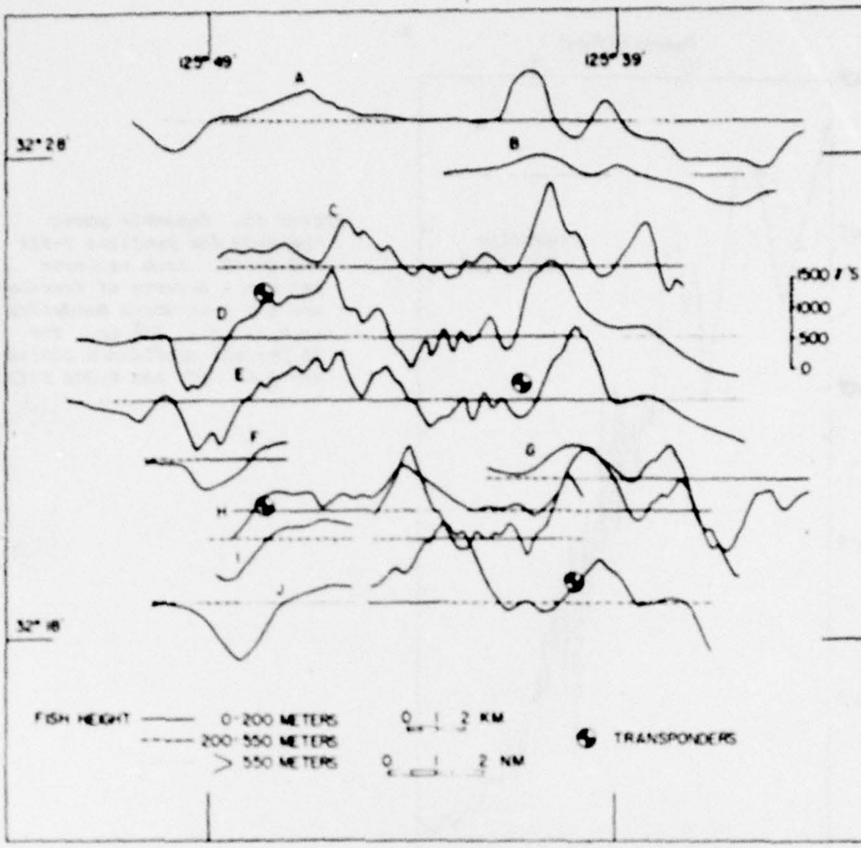

Figure 11. Deep magnetometer profiles from the Luyendyk Hills area projected onto east-west lines. The two profiles analyzed below are the northernmost one and the one immediately below the northeast transponder. Both of these profiles continue east for about 10 kms.

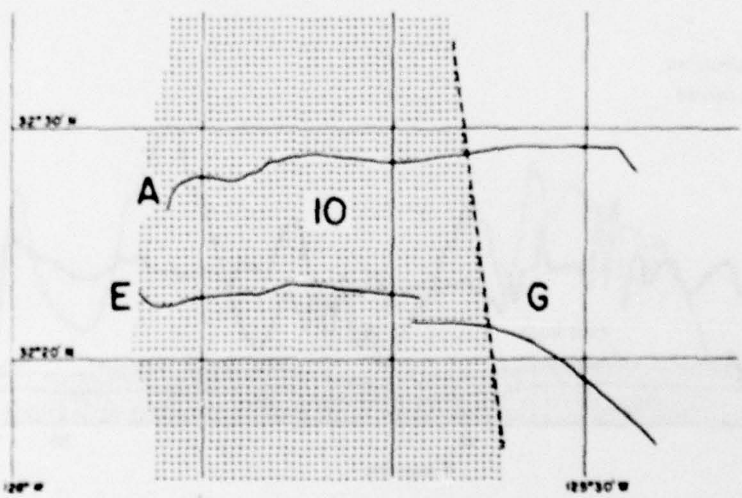

Figure 12. Detail showing tracks of deep profiles in Luyendyk Hills used in this study. T-IIN is profile A, T-IIS is profiles E plus G.

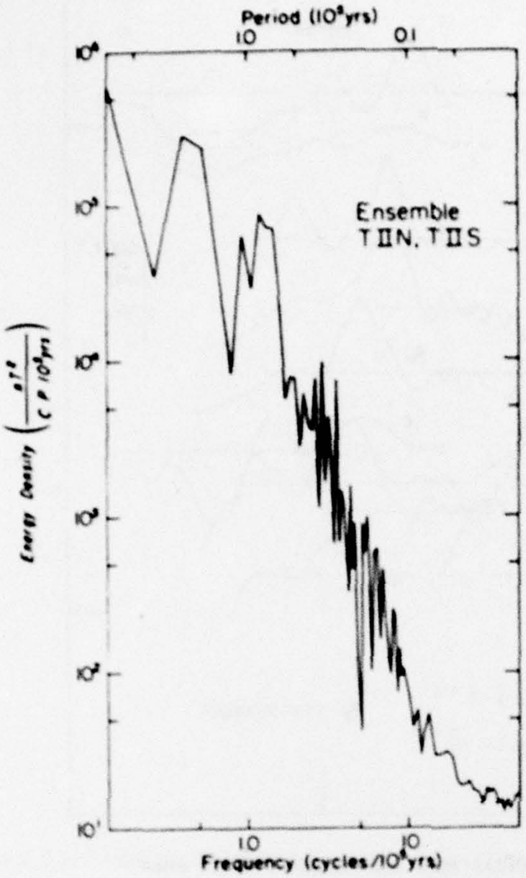

Figure 13. Ensemble power spectrum for profiles T-IIN and T-IIS. Each estimate has n = 4 degrees of freedom and the resolution bandwidth is 0.133 c.p. 10^5 yr. The 95 percent confidence limits are 8.26 S(f) and 0.360 S(f).

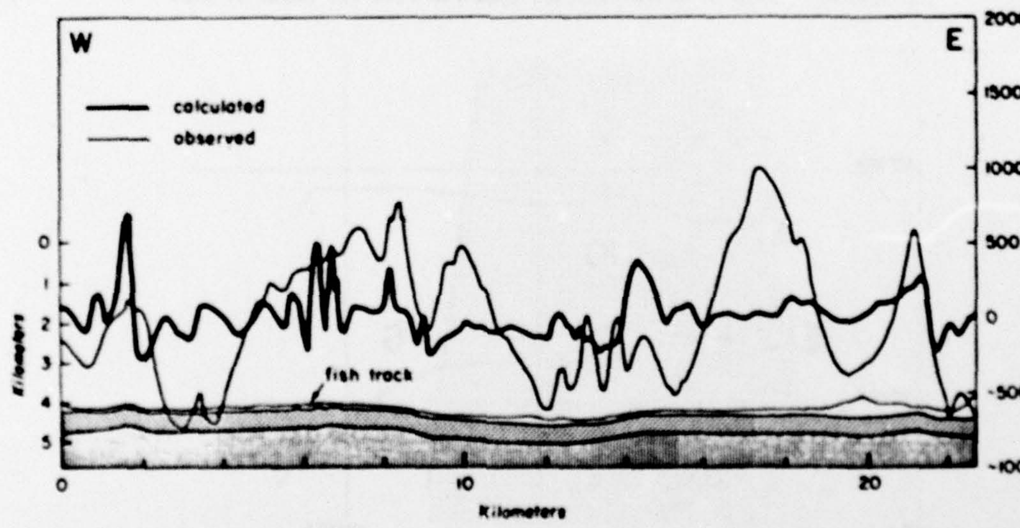

Figure 14. Magnetic anomaly due to uniformly magnetized basement topography for a Luyendyk Hills profile (mainly profile E in Fig. 12). A uniformly magnetized (0.01 cgs, 10 Amp/m) 0.5 kilometer-thick layer is assumed.

TABLE 2

Spreading rates for profiles TIIN, TIIS

Anom	Time, m.y.	TIIN rate	TIIS rate
	31.00		——
	31.16	——	2.11
	31.21		——
		4.63	2.28
	31.36		——
↓	31.50	——	5.3
	31.55		——
10		4.65	4.73
	31.84	——	——
↓		4.6	
	31.92	——	4.63
	31.99		——

Luyendyk Hills - TOW TWO II (T-II2)

These data were originally taken in 1967 before satellite navigation was available aboard SIO ships. Consequently, most of the navigation is a combination of bottom transponder, LORAN fixes, and dead reckoning. Two long profiles were selected from the data base for comparison with the 7 TOW data. These are profiles A and E plus G in Figure 11 and are designated T-IIN and T-IIS. They run from the center (reversed portion) of anomaly 10 east towards anomaly 9 for about 45 km (Figure 12). The profiles are separated from one another by 18 km along strike, and by 16 degrees (ca. 1700 km) from the Gulf of Alaska profiles (10-1 and 10-2). The T-II2 magnetic profiles were reduced to geologic time according to the spreading rates in Table 2. Large discrepancies in rate appear at the younger (east) end. This is due to a conscious effort to match wavelengths on the two profiles. This was necessary because a clear reversal boundary was not found to establish a young control point. At the older end the rates are determined by the youngest edge of anomaly 10 and by the reversal within the anomaly near 31.9 m.y.

The spectral characteristics of the T-II2 time series profiles (Figure 13) are similar to the Gulf of Alaska estimates. Most energy is in periods longer than 10^5 years. It should also be mentioned that the T-II2 profiles were taken about 100 meters or less above basement and thus show more energy at higher frequencies than the 7 TOW data.

The magnetic profiles in the Luyendyk Hills region were combined to produce a composite profile which contained the most short-wavelength anomaly information (taken with magnetometer close to bottom). This profile was analyzed for the contribution of basement topography to the anomaly. The basement topography was determined by airgun reflection and the 3.5 kHz system on the fish. The magnetic anomaly due to basement topography was then calculated using program MAGSYS from SIO. The magnetic layer was assumed 0.5 km thick and magnetized with 20 Amp/m or 0.02 cgs effective susceptibility (about 10 or 0.01 magnetization). Topographic anomalies (Figure 14) are suggested at several places along the profile, but it can generally be seen that the major anomalies (longer wavelength) are not topographically caused.

Coherence Studies of Gulf of Alaska Data

The coherence between two series is analogous to the square of the correlation coefficient between the series (Bendat and Piersol, 1966). It is also defined at discrete frequencies. For a linear system such as

$$x(t) \rightarrow h(t) \rightarrow y(t)$$

the coherence is defined as

$$\gamma^2_{xy}(f) = \frac{|S_{xy}|^2}{S_x S_y} \tag{1}$$

$$0 \leq \gamma^2_{xy}(f) \leq 1,$$

where x is the input, h is the transfer function, and y is the output. S_{xy} is the cross spectrum between x and y and S_x, S_y are power spectra.

For the ideal linear system the coherence is identically one. If it is greater than zero and less than one, then one or more of the following exist (Bendat and Piersol, 1966)

1) extraneous noise is present in the measurements (input or output).

2) the system relating x and y is not linear.

3) $y(t)$ is an output due to an input $x(t)$ as well as to other inputs.

The earth's magnetic field is recorded in the ocean crust during sea floor spreading. If we assume that this can be modelled as a linear system (see Schouten and McCamy, 1972), then $x(t)$ is the earth's field, $h(t)$ is the transfer function of the spreading process and magnetization geometry, and $y(t)$ is the measured magnetic anomaly.

For the profiles 10-1, 10-2, assume that the input field $x(t)$ was the same but the transfer functions and output anomalies are different;

$$x(t) \rightarrow h_1(t) \rightarrow y_1(t) \tag{2}$$
$$x(t) \rightarrow h_2(t) \rightarrow y_2(t)$$

In calculating the coherence between y_1 and y_2, another transfer function is assumed, by definition

$$y_1 \rightarrow h_3 \rightarrow y_2 \tag{3}$$

and

$$\gamma^2_{y_{12}} = \frac{|S_{y_{12}}|^2}{S_{y_1} S_{y_2}}$$

$$\gamma^2_{y_{12}} = \frac{|H_3 S_{y_1}|^2}{S_{y_1} S_{y_2}} \tag{4}$$

This transfer function has no immediate physical meaning, but it is related to h_1 and h_2 as is shown below.

The coherence and phase were calculated between profiles 10-1 and 10-2 using program TIMSAN. The coherence in the program is calculated as the square root of the coherence function above.

$$\gamma_{y_{12}} = \left(\frac{C_{12}^2 + Q_{12}^2}{S_{y_1} \; S_{y_2}} \right)^{1/2} \quad ; \tag{5}$$

and the phase angle between the two series at a given frequency is

$$\phi = \arctan \; (Q_{12}/C_{12}) \quad . \tag{6}$$

Here C_{12} is the cospectrum and Q_{12} is the quadrature (see Hunt, 1977).

The calculated coherence and phase angle degenerate below a period of 10^5 years or a wavelength of 4 km (Figure 15). In the calculation a coherence of 0.8 has a 95 percent probability of being greater than or equal to a true coherence of 0.5 (see caption). From the calculation we can propose that 10-1 and 10-2 are coherent for periods longer than 10^5 years and incoherent for shorter periods.

From the discussion above we can first conclude that one of the three listed reasons explains why $\gamma^2 y_{12} < 1$. But what does it tell us about the presumed linear system between x (earth's field) and y (anomaly field of 10-1 and 10-2)?

We can combine systems in expressions (2) and (3) above and consider again y_1 as input and y_2 as output. In this case take y_1, as input to the left (backwards) into the inverse of h_1 to produce x (x_1) as output. A unit transfer function with no phase shift (h_4) connects "x_1" and "x_2"; x_2 is then input to h_2 to give y_2 as output. This scheme is written as:

$$y_1(t) \rightarrow h_1^{-1}(t) \rightarrow x(t) \rightarrow h_4(t) \rightarrow x(t) \rightarrow h_2(t) \rightarrow y_2(t) \quad . \tag{7}$$

If $h_4(t)$ introduces no phase shift or amplitude distortion, i.e., $H_4^2 = 1$, then

$$H_3 = H_1^{-1} H_2 = \frac{H_2}{H_1} \tag{8}$$

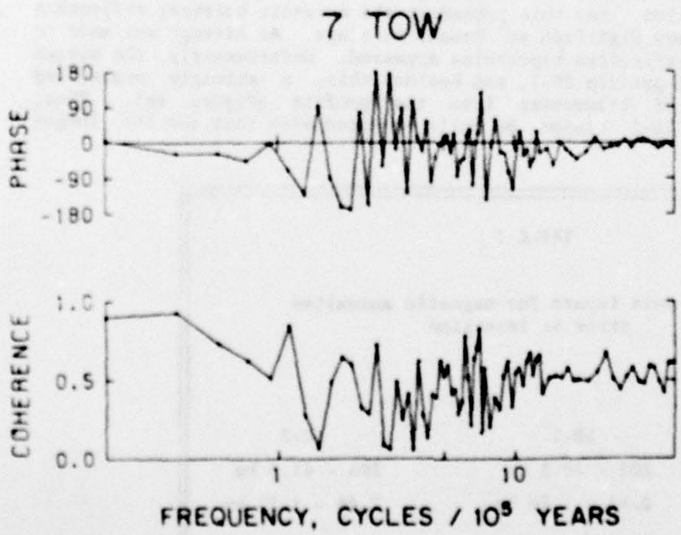

Figure 15. Coherence and phase estimates between profiles 10-1 and 10-2. Each estimate has 8 degrees of freedom. If the estimated coherence is ≥0.8, then the true coherence is ≥0.5 at the 95 percent confidence level (Bendat and Piersol, 1966).

Substitute this into the expression for $\gamma^2_{y_{12}}$ in equation (4);

$$\gamma^2_{y_{12}} = \frac{|H_1^{-1} H_2 \, S_{y_1}|^2}{S_{y_1} \, S_{y_2}} \tag{9}$$

$$\gamma^2_{y_{12}} = \frac{|H_2|^2}{|H_1|^2} \, \frac{S_{y_1}}{S_{y_2}} \tag{10}$$

$$\frac{|H_1|^2}{|H_2|^2} = \gamma^2_{y_{12}} \frac{S_{y_2}}{S_{y_1}} \tag{11}$$

It is equally valid to consider alternatively y_2 as input and y_1 as output. The result is that the numerators and denominators are inter-changed in equation (10) for $\gamma^2 y_{21}$. In this case if $\gamma^2 y_{12} < 1$ we obtain the invalid result that $\gamma^2 y_{21} > 1$ (or vice-versa). This means that since $\gamma^2 \leq 1$ always, equations 10 and 11 are only true for $\gamma^2 = 1$. Also, if $h_4(t)$ does not exist, that is, if x in the first case differs from x in the second case due to noise in one or the other, then equation (7) and below do not hold since a linear system does not relate y_1 and y_2. Equation (11) is the ratio of the convolution theorem applied to profiles 10-1 and 10-2 for the case where S_x is invariant and noise free and only when $\gamma^2 = 1$. Therefore the ratio of the transfer functions can be found where these conditions are met.

Equation (9) shows that the coherence between the outputs y_1 and y_2 (anomaly 10-1 and 10-2) is related to the transfer functions between the earth's field and the respective anomalies. Then for $\gamma^2 < 1$, any of the three above explanations apply to the system linking the earth's field and the anomalies. Intuitively, the most likely causes of $\gamma^2 < 1$ would be noise in the anomalies introduced by noise in the magnetization recorded in the spreading process. Because γ approaches one for periods only greater than 10^5 years in the anomaly 10-1, 10-2 calculations, it appears that a low noise linear system only exists for periods longer than this.

MAGNETIZATION FOR GULF OF ALASKA PROFILES

The magnetic anomaly profiles 10-1 and 10-2 were inverted using the method of Parker and Huestis (1974) in order to investigate correlation between crustal magnetization for the two profiles. For this procedure the acoustic basement reflection time from the airgun profiles was digitized at breaks in slope. An attempt was made to introduce sharp corners where reflection hyperbolae appeared. Unfortunately, the airgun was inoperative for half of profile 10-1, and besides this, a strongly magnetized seamount was encountered 70 kilometers into the profile (Figure 3a). Thus, magnetization solutions for 10-1 cannot be fully compared with that for the longer

TABLE 3

Band-pass tapers for magnetic anomalies prior to inversion

	10-1	10-2
hipass	102 - 20.5 km	205 - 41.0 km
lowpass	2.44 - 1.20 km	2.44 - 1.20 km

profile 10-2. After digitization, reflection times were converted to basement depth beneath the magnetometer, or fish, by assuming a sound speed of 1500 m/sec in water and a gradient of 1.0 sec^{-1} in the sediment. These are the depths shown in Figures 16 and 17.

The magnetic field and the basement depth beneath the magnetometer were then interpolated at an interval of 200 meters for the inversion. Magnetization solutions were computed for a 1 km-thick magnetized layer. Before inversion the magnetic fields were band-pass filtered to insure stability in the solution (Table 3). The magnetization solutions (Figures 16 and 17) faithfully mimic the shapes of the observed magnetic fields (Figures 3a, b). This demonstrates that very little topographic effects are present in the observed fields. Further, the magnetization solutions balance well about zero magnetization strength indicating that little or no annihilator need be added to the results (Parker and Huestis, 1974). The peak amplitudes of magnetization are about 10 Amps/m.

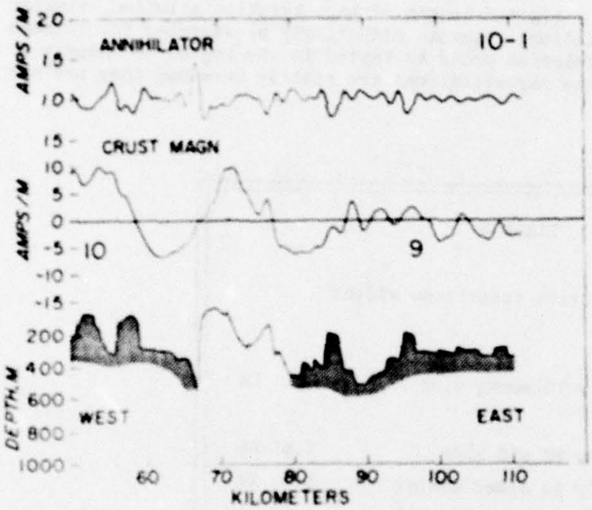

Figure 16. Magnetic inversion study (Parker and Huestis, 1974) for the anomaly in profile 10-1 (Fig. 3a) which has seismic reflection data. The portion of the solution affected by a seamount is shown dotted. Layer thickness is assumed to be one kilometer.

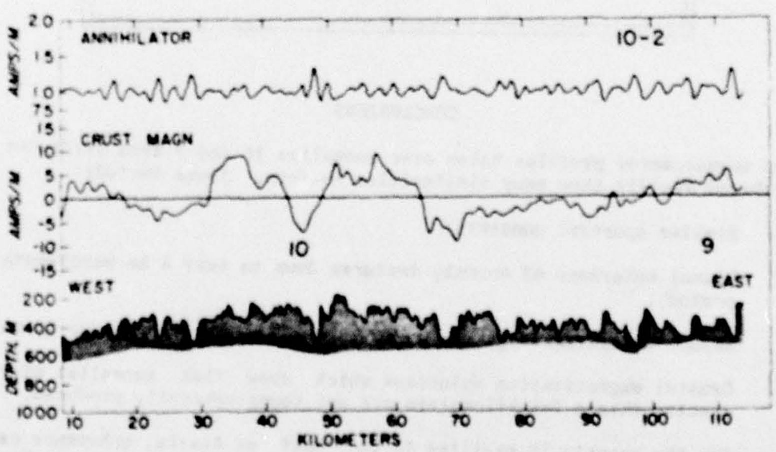

Figure 17. Magnetic inversion study for the anomaly profile 10-2 (Fig. 3b).

The most dramatic result of this analysis is the sharp polarity transitions which define anomaly 10 in contrast to the very weakly defined polarity boundary of anomaly 9. This is also evident in the magnetic field data (Figures 3a, b). Here, although anomaly 9 is well-defined in the magnetic anomaly measured at the sea surface, the anomaly field measured at depth shows no obvious transition. A literal interpretation of the magnetization solutions would indicate that a number of short period reversals mark the older anomaly 9 transition. The fact that this effect is seen in both profiles indicates that it is likely a paleomagnetic field phenomena rather than a geologic effect.

From the crustal magnetization solutions shown in Figures 16 and 17, polarity transition widths can be measured using the criteria of Macdonald (1977). This width is equivalent to the total width of the crustal accretion zone where 90 percent of the magnetized crust is emplaced (Atwater and Mudie, 1973; Macdonald, 1977). The widths vary from 1.35 km to 5.1 km with a median of 3.0 km (Table 4). This width is much larger than the 1.4 km width determined for the East Pacific Rise at 21°N latitude (Macdonald et al., 1979). The results here are in part biased to larger widths because the low-pass cut-off is in fact 1.2 to 2.44 km (Table 3). Thus the widths could be narrower.

Because profile 10-1 only has a limited length of magnetization solution, similar short wavelength magnetization variations cannot effectively be searched for between profiles 10-1 and 10-2. Some correlation could be tested in the region of anomaly 9. The amplitudes and wavelengths of the magnetizations are similar here but they are not in phase between the two profiles.

TABLE 4

Magnetization transition widths

10-1	anomaly 10 young side	5.1 km
10-2	anomaly 10 old side	1.35 km
	anomaly 10 older center	3.0 km
	anomaly 10 younger center	4.0 km
	anomaly 10 young side	1.6 km

CONCLUSIONS

Deep magnetometer profiles taken over anomalies 10 and 9 from different locations in the northeast Pacific show many similarities in form. These include:

1. Similar spectral contents.
2. Visual coherence of anomaly features down to near 4 km wavelength (10^5 year period).
3. Abrupt transition edges to anomaly 10 and diffuse edges for anomaly 9.
4. Crustal magnetization solutions which show that anomalies of wavelengths greater than a few kilometers are not topographically produced.
5. For the anomaly 10 profiles in the Gulf of Alaska, coherence calculations suggest that a low noise linear system exists between the earth's field and crustal magnetization only for periods greater than 10^5 years or wavelengths larger than 4 km.

Correlation between magnetization solutions between profiles cannot yet be meaningfully tested. The sum result of this analysis demonstrates that a signficant portion of the secular variation spectrum is recorded in the ocean crust during sea floor spreading and that it is recorded with a fair degree of fidelity.

ACKNOWLEDGEMENTS

The *Deep Tow group of the Marine Physical Laboratory* is to be thanked for their support over the years. J. D. Mudie and F. N. Spiess aided this project greatly. This work was supported by the Office of Naval Research grants to the Scripps Institution and to the Woods Hole Oceanographic Institution, and by the Academic Senate of U.C. Santa Barbara. Greg Crandall assisted in the data analysis and R. Dodson provided useful discussions on coherence tests. This manuscript was reviewed by Ken Macdonald and Steve Miller.

REFERENCES

Atwater, T. A., and Mudie, J. D., 1973. Detailed near-bottom geophysical study of the Gorda Rise: J. Geophys. Res., v. 78, p. 8665-8686.

Bendat, J. S., and Piersol, A. G., 1966. Measurement and analysis of random data: John Wiley and Sons, New York, 390 pp.

Candie, S. C. and LaBrecque, J. L., 1974. Behavior of earths paleomagnetic fields from small-scale marine magnetic anomalies: Nature, v. 247, p. 26-28.

Heirtzler, J. R., Dickson, G., Herron, E., Pitman, W. III, and Le Pichon, X., 1968. Marine magnetic anomalies, geomagnetic field reversals, and motions of the ocean floor and continents: J. Geophys. Res., v. 73, p. 2119-2136.

Hunt, M., 1977. A program for spectral analysis of time series: WHOI Technical Memoranda No. 2-77, 188 pp.

Klitgord, K. D., Huestis, S. P., Mudie, J. D., and Parker, R. L., 1975. An analysis of near-bottom magnetic anomalies: Seafloor spreading and the magnetized layer: Geophys. J. Roy. Astron. Soc., v. 43, p. 387-424.

Larson, R. L., and Spiess, F. N., 1969. The East Pacific Rise crest: A near-bottom geophysical profile: Science, v. 163, p. 66-67.

Larson, R. L., Larson, P., Mudie, J. D., and Spiess, F. N., 1974. Models of near-bottom magnetic anomalies on the East Pacific Rise crest at 21°N: J. Geophys. Res., v. 79, p. 2686-2689.

Luyendyk, B. P., 1969. Origin of short wavelength magnetic lineations observed near the ocean bottom: J. Geophys. Res., v. 74, p. 4869-4881.

Luyendyk, B. P., 1970. The origin and history of abyssal hills in the northeast Pacific: Bull. Geol. Soc. Amer., v. 81, p. 3411-3416.

Luyendyk, B. P., Mudie, J. D., and Harrison, C. G. A., 1968. Lineation of magnetic anomalies in the northeast Pacific observed near the ocean bottom: J. Geophys. Res., v. 74, p. 5951-5957.

Macdonald, K. C., 1977. Near-bottom magnetic anomalies, asymmetric spreading, oblique spreading, and tectonics of the Mid-Atlantic Ridge near lat. 37°N: Bull. Geol. Soc. Amer., v. 88, p. 541-555.

Macdonald, K. C., Miller, S. P., Huestis, S., and Spiess, F. N., 1979. Three-dimensional modelling of a Brunhes/Matuyama reversal boundary from inversion of deep-tow measurements: J. Geophys. Res., in press.

McCullough, J. R., 1968. WHOI Technical Memoranda No. 68-78.

Menard, H. W. and Atwater, T. A., 1968. Changes in direction of sea floor spreading: Nature, v. 219, p. 463-467.

Otnes, R. K., and Enochson, L., 1978. Applied time series analysis (vol. I): John Wiley and Sons, New York, 449 pp.

Parker, R. L., and Huestis, S., 1974. The inversion of magnetic anomalies in the presence of topography: J. Geophys. Res., v. 79, p. 1587-1593.

Schouten, H., and McCamy, K., 1972. Filtering marine magnetic anomalies: J. Geophys. Res., v. 77, p. 7089-7099.

Spiess, F. N., Grow, J., Luyendyk, B. P., and Mudie, J. D., 1970. Seven Tow, Leg 8 cruise report: SIO REF 70-31, 7 pp.

Spiess, F. N., and Tyce, R. C., 1973. Marine Physical Laboratory deep tow system: SIO REF 73-4, 37 pp.

Stallings, C. B., 1966. Proc. AFIPS Conf. 29, p. 549-561.

DISTRIBUTION LIST

Chief of Naval Research
Department of the Navy
Arlington, Virginia 22217

Code 200	(1)
Code 222	(2)
Code 102 D1	(1)
Code 1020S	(1)
Code 460	(1)
Code 480	(1)
Code 481	(1)
Code 482	(1)
Code 483	(1)
Code 484	(1)
Code 485	(1)
Code 486	(1)

Director
Office of Naval Research
Branch Office
1030 East Green Street
Pasadena, California 91101 (1)

Commander
Naval Sea Systems Command
Washington, D. C. 20362

Code 03E	(1)
Code 034	(1)
Code 0342	(1)
Code 036	(1)
Code 06H1	(1)
Code 06H1-4	(1)
Code 06H2-5	(1)
Code 09G3	(1)
Code 92	(1)
Code 662C14	(1)
PMS 395	(1)
PMS 395-A4	(1)
PMS 395-A1	(1)
PMS 402-B	(1)
Code 03423 (Mr. Francis J. Romano)	(1)

Commander
Naval Air Systems Command
Washington, D. C. 20361

Code 370	(1)
Code 264	(1)

Commander
Naval Electronics Systems Command
Washington, D. C. 20360

Code PME-124	(1)
Code PME-124-20	(1)
Code PME-124-30	(1)
Code PME-124-60	(1)
Code 320	(1)
Code 3202	(1)

Chief of Naval Material
Department of the Navy
Washington, D. C. 20360

Code 0345	(1)
Code 03T	(1)
Code 031	(1)
Code ASW-00	(1)
Code ASW-11	(1)
Code ASW-13	(1)
Code ASW-14	(1)

Chief of Naval Operations
Department of the Navy
Washington, D. C. 20350

Code Op 03	(1)
Code Op 32	(1)
Code Op 098	(1)
Code Op 981	(1)
Code Op 02	(1)
Code Op 095	(1)
Code Op 955F	(1)
Code Op 23	(1)
Code Op 967	(1)

Commanding Officer
Naval Ocean Research Development
Activity (NORDA)
National Space Technology Laboratories
Bay St. Louis, Mississippi 39529

Code 100	(1)
Code 110	(1)
Code 200	(1)
Code 300	(1)
Code 330	(1)
Code 340	(1)
Code 350	(1)
Code 360	(1)
Code 500	(1)
Code 600	(1)

Defense Advanced Research Projects Agency
1400 Wilson Boulevard
Arlington, Virginia 22209
Dr. Phillip Selwyn (1)

Director
U.S. Naval Oceanographic Office
National Space Technology Laboratories
Bay St. Louis, Mississippi 39522

Wilburt H. Geddes	(1)
Russ Mooney	(1)

Director
Defense Research & Engineering
The Pentagon - 3D1048
Washington, D. C. 20301
Assistant Director (Ocean Control) (1)

Director
Strategic Systems Projects Office (PM-1)
Department of the Navy
Washington, D. C. 20360
Code NSP-20 (1)

Commander Operational Test &
Evaluation Force
U. S. Naval Base
Norfolk, Virginia 23511 (1)

Commander, Submarine Force
U. S. Pacific Fleet
Fleet Post Office
San Francisco, California 96601 (1)

Commander
Submarine Group FIVE
Fleet Station Post Office
San Diego, California 92132 (1)

Commander
Third Fleet
U. S. Pacific Fleet, FPO
San Francisco, California 96610 (1)

Commander
Submarine Development Group ONE
Fleet Post Office
San Diego, California 92132 (1)

Commander
Submarine Development Group TWO
Naval Submarine Base - New London
Groton, Connecticut 06340 (1)

Commander, Surface Force
U. S. Atlantic Fleet
Norfolk, Virginia 23511 (1)

Commander, Surface Force
U. S. Pacific Fleet
San Diego, California 92155 (1)

Reprint Custodian
Department of Nautical Science
U. S. Merchant Marine Academy
Kings Point, New York 11024 (1)

Deputy Commander
Operational Test & Evaluation Force, Pacific
U. S. Naval Air Station
San Diego, California 92135 (1)

Commanding Officer
Civil Engineering Laboratory
Naval Construction Battalion Center
Port Hueneme, California 93043
Code L40 (1)
Code L42 (1)

Commander
Naval Ship Research & Development Center
Bethesda, Maryland 20084 (1)

Naval Facilities Engineering Command
Washington, D. C. 20390
Code 03 (1)
Code 032C (1)

Commanding Officer
U. S. Naval Air Development Center
Attention Jim Howard
Warminster, Pennsylvania 18974 (1)

Commander
Naval Ocean Systems Center
San Diego, California 92152
Code 00 (1)
Code 01 (1)
Code 52 (1)
Code 531 (1)
Code 5301 (1)
Code 71 (1)
Code 72 (1)
Code 614 (1)

Officer In Charge
Naval Ship Research & Development Center
Annapolis, Maryland 21402 (1)

Commanding Officer
Naval Coastal Systems Laboratory
Panama City, Florida 32401 (1)

Commander
Naval Surface Combat Systems Center
White Oak
Silver Spring, Maryland 20910 (1)

Director of Research
U. S. Naval Research Laboratory
Washington, D. C. 20375
Code 2620 (1)
Code 2627 (1)
Code 8000 (1)
Code 8100 (1)

Commanding Officer
Naval Underwater Systems Center
Newport, Rhode Island 20844 (1)
John D'Albora (1)

Commanding Officer
Naval Training Equipment Center
Orlando, Florida 32813
Tech Library (1)

Superintendent
U. S. Naval Postgraduate School
Monterey, California 93940 (1)

Officer In Charge
Naval Underwater Systems Center
New London Laboratory
New London, Connecticut 06320

Code 900	(1)
Code 905	(1)
Code 910	(1)
Code 930	(1)
Code 960	(1)

Chief Scientist
Navy Underwater Sound Reference Division
U. S. Naval Research Laboratory
P.O. Box 8337
Orlando, Florida 32806 (1)

Director
Defense Documentation Center
(TIMA), Cameron Station
5010 Duke Street
Alexandria, Virginia 22314 (12)

Executive Secretary, Naval Science Board
National Academy of Sciences
2101 Constitution Avenue, N.W.
Washington, D. C. 20418 (1)

Supreme Allied Commander
U. S. Atlantic Fleet
ASW Research Center
APO
New York, New York 09019
Via: ONR 210
CNO OP092D1
Secretariat of Military
Information Control
Committee (1)

Assistant Secretary of the Navy
(Research Engineering & Systems)
Department of the Navy
Washington, D. C. 20350 (1)

National Oceanic & Atmospheric
Administration
Ocean Engineering Office
6001 Executive Boulevard
Rockville, Maryland 20852 (1)

Director of Naval Warfare Analysis
Institute of Naval Studies
1401 Wilson Boulevard
Arlington, Virginia 22209 (1)

Institute for Defense Analyses
400 Army-Navy Drive
Arlington, Virginia 22202 (1)

Director
Woods Hole Oceanographic Institution
Woods Hole, Massachusetts 02543 (1)

Meterorological & Geo-
Astrophysical Abstracts
301 E. Capitol Street
Washington, D. C. 20003 (1)

Director
Applied Physics Laboratory
University of Washington
1013 East 40th Street
Seattle, Washington 98105

Director
Lamont-Doherty Geological Observatory
Torrey Cliff
Palisades, New York 10964

Director
College of Engineering
Department of Ocean Engineering
Florida Atlantic University
Boca Raton, Florida 33431 (1)

Director
Attention Dr. J. Robert Moore
Institute of Marine Science
University of Alaska
Fairbanks, Alaska 99701 (1)

Director
Applied Physics Laboratory
Johns Hopkins University
Johns Hopkins Road
Laurel, Md. 20810
Attention J. R. Austin (1)

Director
Applied Research Laboratory
Pennsylvania State University
P.O. Box 30
State College, Pennsylvania 16802 (1)

Director
University of Texas
Applied Research Laboratory
P.O. Box 8029
Austin, Texas 78712 (1)

STOIAC
Battelle Columbus Laboratories
505 King Avenue
Columbus, Ohio 43201 (1)

Director
Institute of Ocean Science & Engineering
Catholic University of America
Washington, D. C. 20017 (1)

Director
Marine Research Laboratories
c/o Marine Studies Center
University of Wisconsin
Madison, Wisconsin 53706 (1)

Office of Naval Research
Resident Representative
c/o University of California, San Diego
La Jolla, California 92093 (1)

University of California, San Diego
Marine Physical Laboratory Branch Office
La Jolla, California 92093 (5)

Commanding Officer
Office of Naval Research
Branch Office
London, England U. K.
Box 39 FPO New York 09510 (2)

National Science Foundation
Washington, D. C. 20550 (1)

ONR/MPL General January 1979

Marine Physical Laboratory
MPL-U-60/79

IS MAGNETIC SECULAR VARIATION RECORDED IN THE OCEAN CRUST: ANALYSIS OF DEEP TOWED MAGNETIC ANOMALIES MEASURED ON CRUISES TOW TWO II AND SEVEN TOW by Bruce P. Luyendyk, University of California, Santa Barbara, Department of Geological Sciences, Santa Barbara, California 93106. SIO Reference 79-20, 1 October 1979.

Deeply towed marine magnetometer profiles over anomalies 10 and 9 in the Gulf of Alaska, and number 10 off California, were studied for correlation of short wavelength (short period) features. It is proposed that part of the (dipole) secular variation spectrum is recorded with some fidelity during sea floor spreading. Statistical and model studies suggest that topographic effects are not significant in the data analyzed. Agreement between profiles degenerates at periods shorter than 10 years (wavelengths less than 4 km) and coherence tests suggest that a linear system related the earth's field and ocean crust magnetization only at periods longer than this. One striking observation is that the polarity transitions to anomaly 10 are very sharp but the anomaly 9 transition is broad and cannot easily be located in the deep magnetometer profiles.

IIIc. Geomagnetics

B. P. Luyendyk

Sponsored by the
Office of Naval Research
N00014-69-A-0200-6002

UNCLASSIFIED

Marine Physical Laboratory
MPL-U-60/79

IS MAGNETIC SECULAR VARIATION RECORDED IN THE OCEAN CRUST: ANALYSIS OF DEEP TOWED MAGNETIC ANOMALIES MEASURED ON CRUISES TOW TWO II AND SEVEN TOW by Bruce P. Luyendyk, University of California, Santa Barbara, Department of Geological Sciences, Santa Barbara, California 93106. SIO Reference 79-20, 1 October 1979.

Deeply towed marine magnetometer profiles over anomalies 10 and 9 in the Gulf of Alaska, and number 10 off California, were studied for correlation of short wavelength (short period) features. It is proposed that part of the (dipole) secular variation spectrum is recorded with some fidelity during sea floor spreading. Statistical and model studies suggest that topographic effects are not significant in the data analyzed. Agreement between profiles degenerates at periods shorter than 10 years (wavelengths less than 4 km) and coherence tests suggest that a linear system related the earth's field and ocean crust magnetization only at periods longer than this. One striking observation is that the polarity transitions to anomaly 10 are very sharp but the anomaly 9 transition is broad and cannot easily be located in the deep magnetometer profiles.

IIIc. Geomagnetics

B. P. Luyendyk

Sponsored by the
Office of Naval Research
N00014-69-A-0200-6002

UNCLASSIFIED

Marine Physical Laboratory
MPL-U-60/79

IS MAGNETIC SECULAR VARIATION RECORDED IN THE OCEAN CRUST: ANALYSIS OF DEEP TOWED MAGNETIC ANOMALIES MEASURED ON CRUISES TOW TWO II AND SEVEN TOW by Bruce P. Luyendyk, University of California, Santa Barbara, Department of Geological Sciences, Santa Barbara, California 93106. SIO Reference 79-20, 1 October 1979.

Deeply towed marine magnetometer profiles over anomalies 10 and 9 in the Gulf of Alaska, and number 10 off California, were studied for correlation of short wavelength (short period) features. It is proposed that part of the (dipole) secular variation spectrum is recorded with some fidelity during sea floor spreading. Statistical and model studies suggest that topographic effects are not significant in the data analyzed. Agreement between profiles degenerates at periods shorter than 10 years (wavelengths less than 4 km) and coherence tests suggest that a linear system related the earth's field and ocean crust magnetization only at periods longer than this. One striking observation is that the polarity transitions to anomaly 10 are very sharp but the anomaly 9 transition is broad and cannot easily be located in the deep magnetometer profiles.

IIIc. Geomagnetics

B. P. Luyendyk

Sponsored by the
Office of Naval Research
N00014-69-A-0200-6002

UNCLASSIFIED

Marine Physical Laboratory
MPL-U-60/79

IS MAGNETIC SECULAR VARIATION RECORDED IN THE OCEAN CRUST: ANALYSIS OF DEEP TOWED MAGNETIC ANOMALIES MEASURED ON CRUISES TOW TWO II AND SEVEN TOW by Bruce P. Luyendyk, University of California, Santa Barbara, Department of Geological Sciences, Santa Barbara, California 93106. SIO Reference 79-20, 1 October 1979.

Deeply towed marine magnetometer profiles over anomalies 10 and 9 in the Gulf of Alaska, and number 10 off California, were studied for correlation of short wavelength (short period) features. It is proposed that part of the (dipole) secular variation spectrum is recorded with some fidelity during sea floor spreading. Statistical and model studies suggest that topographic effects are not significant in the data analyzed. Agreement between profiles degenerates at periods shorter than 10 years (wavelengths less than 4 km) and coherence tests suggest that a linear system related the earth's field and ocean crust magnetization only at periods longer than this. One striking observation is that the polarity transitions to anomaly 10 are very sharp but the anomaly 9 transition is broad and cannot easily be located in the deep magnetometer profiles.

IIIc. Geomagnetics

B. P. Luyendyk

Sponsored by the
Office of Naval Research
N00014-69-A-0200-6002

UNCLASSIFIED